

Control of Cellular Bcl-x_L Levels by Deamidation-Regulated Degradation

So Hee Dho^{1,2}, Benjamin E. Deverman^{1‡}, Carlo Lapid³, Scott R. Manson¹, Lu Gan¹, Jacob J. Riehm¹, Rajeev Aurora⁴, Ki-Sun Kwon^{2*}, Steven J. Weintraub^{1,5,6*}

1 Division of Urology and The Alvin J. Siteman Cancer Center, Washington University School of Medicine, Saint Louis, Missouri, United States of America, **2** Laboratory of Cell Signaling, Aging Research Center, Korea Research Institute of Bioscience and Biotechnology, Yusong, Daejeon, Korea, **3** Department of Biology, Washington University, Saint Louis, Missouri, United States of America, **4** Department of Molecular Microbiology and Immunology, Saint Louis University School of Medicine, Saint Louis, Missouri, United States of America, **5** Department of Internal Medicine, Washington University School of Medicine, Saint Louis, Missouri, United States of America, **6** Department of Internal Medicine, St. Louis VA Medical Center–John Cochran Division, Saint Louis, Missouri, United States of America

Abstract

The cellular concentration of Bcl-x_L is among the most important determinants of treatment response and overall prognosis in a broad range of tumors as well as an important determinant of the cellular response to several forms of tissue injury. We and others have previously shown that human Bcl-x_L undergoes deamidation at two asparaginyl residues and that DNA-damaging antineoplastic agents as well as other stimuli can increase the rate of deamidation. Deamidation results in the replacement of asparaginyl residues with aspartyl or isoaspartyl residues. Thus deamidation, like phosphorylation, introduces a negative charge into proteins. Here we show that the level of human Bcl-x_L is constantly modulated by deamidation because deamidation, like phosphorylation in other proteins, activates a conditional PEST sequence to target Bcl-x_L for degradation. Additionally, we show that degradation of deamidated Bcl-x_L is mediated at least in part by calpain. Notably, we present sequence and biochemical data that suggest that deamidation has been conserved from the simplest extant metazoans through the human form of Bcl-x_L, underscoring its importance in Bcl-x_L regulation. Our findings strongly suggest that deamidation-regulated Bcl-x_L degradation is an important component of the cellular rheostat that determines susceptibility to DNA-damaging agents and other death stimuli.

Citation: Dho SH, Deverman BE, Lapid C, Manson SR, Gan L, et al. (2013) Control of Cellular Bcl-x_L Levels by Deamidation-Regulated Degradation. PLoS Biol 11(6): e1001588. doi:10.1371/journal.pbio.1001588

Academic Editor: Douglas R. Green, St. Jude Children's Research Hospital, United States of America

Received: November 25, 2012; **Accepted:** May 7, 2013; **Published:** June 25, 2013

This is an open-access article, free of all copyright, and may be freely reproduced, distributed, transmitted, modified, built upon, or otherwise used by anyone for any lawful purpose. The work is made available under the Creative Commons CC0 public domain dedication.

Funding: This work was supported by grants to SJW from the US NIH and grants to K-SK from National Research Foundation of Korea (20110030133 and 20110027762) and from the National R&D Program for Cancer Control, Ministry of Health & Welfare, Korea (12201901-14924). The funders had no role in study design, data collection and analysis, decision to publish, or preparation of the manuscript.

Competing Interests: The authors have declared that no competing interests exist.

Abbreviations: MEF, mouse embryo fibroblast; pRb, retinoblastoma protein.

* E-mail: kwonks@kribb.re.kr (K-SK); sjweintraub@gmail.com (SJW)

‡ Current address: Division of Biology, California Institute of Technology, Pasadena, California, United States of America

Introduction

The Bcl-2 proteins are grouped into those that promote cell survival and those that promote programmed cell death [1]. It is thought that the balance of activity of these two groups of proteins serves as a rheostat that determines whether the cell lives or dies [2]. The activity of the prosurvival Bcl-2 proteins is normally dominant in a cell. Most antineoplastic agents and other proapoptotic agents induce changes in Bcl-2 proteins that tip the balance towards the prodeath activity [3]. Importantly, this may involve a decrease in the activity of prosurvival proteins, an increase in the activity of prodeath proteins, or a combination of both.

There is substantial evidence that the level of the prosurvival Bcl-2 family protein Bcl-x_L is one of the most important cellular determinants of patient outcome in a broad range of tumors. For example, increased Bcl-x_L expression portends a worse prognosis in pancreatic cancer [4], thyroid cancer [5], follicular lymphoma [6], ovarian cancer [7,8], hepatocellular carcinoma [9], and prostate cancer [10] and it has been specifically shown that increased levels of Bcl-x_L correlate with treatment failure in

thyroid cancer [5], ovarian cancer [8], and oropharyngeal cancer [11]. In support of a functional role for Bcl-x_L in determining the prognosis and treatment response of patients with these cancers are the findings that (i) there is a “striking” correlation between resistance to treatment with a panel of 122 chemotherapeutic agents and Bcl-x_L expression levels when assessed in 60 different types of tumor cells [12]; (ii) overexpression of Bcl-x_L confers a multidrug resistance phenotype to tumor cells [13]; (iii) a small molecule or antisense that selectively inhibits Bcl-x_L increases sensitivity to chemotherapy in vivo [14,15]; (iv) at least in some cells, there is a *bcl-x* gene-dosage effect for resistance to DNA-damaging agents [16]; and (v) increased Bcl-x_L expression increases susceptibility to carcinogen-induced tumor formation in mice [17]. When considered together, these findings suggest that tumor cell Bcl-x_L levels have an important functional role in determining patient outcome.

The expression level of Bcl-x_L is also important in determining the extent of damage in certain forms of tissue injury; in fact, Bcl-x_L levels may be upregulated to protect against certain forms of injury. For example, liver cells with decreased Bcl-x_L levels

Author Summary

Cellular levels of the pro-survival protein Bcl-x_L are an important determinant of cellular susceptibility to many death stimuli, including most cancer therapies. We previously showed that human Bcl-x_L undergoes deamidation – the conversion of two neutral asparaginyl side-chains into negatively charged aspartyl side-chains – a process that occurs spontaneously but is accelerated by the treatment of tumor cells with DNA-damaging agents. Here, we show that deamidation activates a hitherto undetected signal sequence within Bcl-x_L that targets it for degradation by a pathway involving the proteolytic enzyme calpain. This increased degradation of Bcl-x_L, and the consequent enhanced cellular susceptibility to programmed cell death, may contribute to the ability of DNA-damaging agents to kill tumors. We also demonstrate that deamidation of Bcl-x_L has likely been conserved from the simplest metazoans to humans, underscoring the importance of deamidation in the regulation of Bcl-x_L.

demonstrate increased susceptibility to injury [17,18]; conversely, transgenic overexpression of Bcl-x_L protects against liver injury [19]. In this context, it is intriguing that hepatic Bcl-x_L expression is upregulated in response to liver injury [20,21]. Similarly, Bcl-x_L levels are upregulated in the esophageal mucosa in response to chronic acid reflux [22]. It is likely that the increased Bcl-x_L in these and other instances protects against tissue injury.

The findings outlined above underscore the importance of understanding the mechanisms by which Bcl-x_L levels are regulated. We and others have previously shown that two asparagines in human Bcl-x_L undergo deamidation to aspartyl or isoaspartyl residues and that the rate of deamidation of these asparagines increases in susceptible tumor cells that are treated with DNA-damaging agents [16,23,24]. We now present evidence that asparagine deamidation has been conserved in Bcl-x_L-like proteins from the simplest extant metazoans through the human form of Bcl-x_L. This extent of conservation suggests that deamidation has a critical role as a regulatory posttranslational modification of Bcl-x_L. Indeed, we demonstrate here that the rate of deamidation dynamically modulates the cellular level of Bcl-x_L because deamidation is a continuous but regulated process that, like phosphorylation in other proteins, activates a conditional PEST sequence to target Bcl-x_L for degradation. Importantly, we show that in susceptible tumor cells, DNA-damaging agents decrease Bcl-x_L levels, which increases cellular susceptibility to death signaling, because these agents induce an increase in the rate of deamidation of Bcl-x_L and, consequently, an increase in the rate of degradation of Bcl-x_L. In contrast, however, we have previously shown that at least in some nontransformed cells the increased rate of Bcl-x_L deamidation and consequent degradation that would otherwise occur upon treatment with DNA-damaging antineoplastic agents is suppressed by p53-retinoblastoma protein (pRb) signaling; hence, Bcl-x_L levels remain static in these cells when they are treated with DNA-damaging antineoplastic agents [16]. Therefore, Bcl-x_L deamidation is a regulatable process and certain stimuli can shift the balance of cellular pro-survival and pro-death activity by altering the rate of Bcl-x_L deamidation.

Results

Bcl-x_L Deamidation Is Highly Conserved

Asparagine deamidation is a nonenzymatic posttranslational modification. Although asparagine deamidation occurs spontane-

ously, its rate can be regulated by changes in the pH, ionic composition, or temperature of the surrounding cellular microenvironment [25]. An asparagine is most susceptible to deamidation when it is immediately followed by a glycine in a conformationally flexible region of a protein because deamidation is initiated when the peptide bond nitrogen of the N+1 amino acid attacks the carbonyl carbon of the asparagine side chain—this is facilitated by the reduced steric hindrance of glycine and flexibility of the surrounding sequence [25].

Human Bcl-x_L has a large conformationally flexible region between the BH4 and BH3 domains that is referred to as its flexible loop (Figure 1A) [26] and we have previously demonstrated that two asparagines that are immediately followed by glycines that lie within the flexible loop undergo deamidation [16]. We now report that Bcl-x_L-like proteins from sponge through human contain asparagine-glycine sequences within a region that is predicted to be conformationally flexible between the BH4 and BH3 domains (Figure 1B) [27,28]. The widespread presence of these asparagine-glycine sequences in the flexible region is striking as there is no other obvious sequence similarity within this region across all species (Figure 1B), and it suggests that the presence of an asparagine-glycine sequence per se is a conserved feature of the flexible loop of Bcl-x_L. Additionally, there are a number of species that express Bcl-x_L-like proteins that have a long flexible region immediately upstream of the BH4 domain (Figure 2A), and we found that each of these proteins contains an asparagine-glycine sequence in this region (Figure 2B), suggesting that an asparagine-glycine sequence within a flexible region is a conserved feature of Bcl-x_L.

To objectively assess whether asparagine-glycine sequences are indeed a conserved feature of the Bcl-x_L flexible loop, we performed a de novo analysis of an independently assembled group of Bcl-x_L-like proteins, the Bcl-x_L homology group of the Bcl-2 family database [29], using the MEME conserved motif discovery algorithm [30]. MEME is a widely used tool that searches for sequences that are reiterant within an input group of proteins and assigns each an *E*-value, a statistical estimate of the probability that the sequence would occur with an equal or greater frequency than it occurs in the input group of proteins if the amino acids of the proteins were positionally randomized [31]. Sequences with *E*-values of less than 1×10^{-2} likely represent conserved, and therefore functional, motifs [32].

In a dataset consisting of the sequences of the entire region between the BH4 and BH3 domains from all of the members of the Bcl-x_L homology group in the Bcl-2 database (Figure S1) [29], the asparagine-glycine dipeptide occurs in more sequences and with a greater frequency than any other dipeptide and it is assigned an *E*-value of 2.0×10^{-3} by MEME. Furthermore, almost half (91/187) of the asparagines in the dataset are a component of an asparagine-glycine sequence. These findings strongly suggest that there is selective pressure to maintain the asparagine-glycine sequence in this region. This implies that deamidation is a conserved feature of the Bcl-x_L flexible loop because, to our knowledge, the only function asparagine-glycine dipeptides could have in this context is to serve as deamidation sites. We examined this further by determining if deamidation occurs within three flexible loops in which the asparagine-glycine sequences are surrounded by widely disparate sequences: the flexible loops in the human, *Xenopus laevis*, and zebrafish forms of Bcl-x_L (Figure 3A).

We have previously demonstrated that two asparagines in the flexible loop of human Bcl-x_L undergo deamidation [16]. Deamidation is readily detected in human Bcl-x_L because the deamidated forms migrate more slowly than the native form during SDS-PAGE [16]. The more slowly migrating forms do not

A**B**

Sponge	44-IKLNGYAGNGRTSHTRNRLTND-65	<i>Suberites domuncula</i>
	70-MSVNGYTDVLPGLRKRKPRKER-91	<i>Geodia cydonium</i>
	47-TRLNGFRSSVVEAAARRFDDNP-68	<i>Oscarella carmela</i>
	66-VKLNGYTTGHVEPIFSSETNRK-87	<i>Amphimedon queenslandica</i>
Mollusk	24-QWENGPAQRKNNKVFQAVRKLK-45	<i>Crassostrea gigas</i> (Pacific oyster)
	40-VWENGRQGNVTPNSVEA -56	<i>Aplysia californica</i> (sea hare)
Fish	37-TQSNNGTFNGASPGTTPPAPSQHQ-58	<i>Tetraodon nigroviridis</i> (pufferfish)
	51-THSNNGTFNGTSPGTPPASPQLLQ-72	<i>Gasterosteus aculeatus</i> (stickleback)
	44-AIANGSLGNNRNGRSNLGMPSS-62	<i>Oncorhynchus mykiss</i> (rainbow trout)
	41-AIANGSLGNNRNGRSNLGKPPSS-62	<i>Salmo salar</i> (salmon)
	41-AIANGSLGNNRNGRSNLGMPSS-62	<i>Oncorhynchus nerka</i> (sockeye salmon)
	50-THANGTFTGTSPGTPPVSPLRQ-71	<i>Odontesthes bonariensis</i> (silverside)
	50-IGNNGLRLNDGNGNGQLAPSPT-71	<i>Gadus morhua</i> (cod)
	44-SPVNGSVENDRNCIGSLGISSS-65	<i>Osmerus mordax</i> (smelt)
	47-AARNGLLASKNTSGQPGTSSSS-65	<i>Dicentrarchus labrax</i> (sea bass)
	39-AEENGEAGAAGATTLVNGTMNRT-	<i>Danio rerio</i> (zebrafish)
	NASSTGTPPQSPASSPQRQTNG-82	
	39-AEENGEAGAAGTTLVNGSMNRT-	<i>Rutilus rutilus</i> (roach minnow)
	PPRSPASSPQHQTNGTGGLDAV-82	
	39-AEENGEAGAAGTTLVNGSMNRT-	<i>Pimephales promelas</i> (scrapemouth)
	PPRSPTSSPQHQTNGTGGLDAV-82	
Amphibian	34-AISNGTSTSERPGEATQGIVE-55	<i>Xenopus laevis</i>
	34-GVNSGSSEGPATQGIVGEEVL-55	<i>Xenopus (Silurana) tropicalis</i>
Reptile	24-SVPNGSPSWHPGASHVVNGAAG-45	<i>Trachemys scripta elegans</i> (turtle)
	44-NTLNGSPSWHPSHVINNGASE-65	<i>Anolis carolinensis</i> (anole-lizard)
Bird	46-GVLNGSPSWHAATSHIVNGATV-67	<i>Lonchura striata</i> (striated finch)
	46-GVLNGSPSWHAATSHIVNGATV-67	<i>Taeniopygia guttata</i> (zebra finch)
	35-SVLNGSPSWHPPAGHVVNGATV-56	<i>Lagopus lagopus</i> (willow grouse)
	45-SVLNGSPSWHPPAGHVVNGATV-66	<i>Gallus gallus</i> (chicken)
	45-SVLNGSPSWHPPAGHVVNGAAV-66	<i>Meleagris gallopavo</i> (turkey)
Mammal	43-STVNGSPSWHPADSRVSGATG-64	<i>M. domestica</i> (opossum-a marsupial)
	43-STVNGSPSWHPADSRAGSGATG-64	<i>S. crassicaudata</i> (dunnart-marsupial)
	49-SAINGNPSWHLADSPAVNGATG-70	<i>Cricetulus griseus</i> (hamster)
	49-SAINGNPSWHLADSPAVNGATG-70	<i>Mus musculus</i> (mouse)
	49-SAINGNPSWHLADSPAVNGATG-70	<i>Rattus norvegicus</i> (rat)
	29-SAINGNPSWHLADSPAINGATG-50	<i>S. tridecemlineatus</i> (ground squirrel)
	49-SAINGNPSWHLADSPAVNGATG-70	<i>Ailuropoda melanoleuca</i> (panda)
	49-SAINGNASWHLADSPAVNGATG-70	<i>Bos taurus</i> (cow)
	49-SAINGNPSWHLADSPAVNGATG-70	<i>Canis lupus familiaris</i> (dog)
	49-SAINGNPSWHLADSPGTGNGATG-70	<i>Equus caballus</i> (horse)
	49-SAINGNPSWHLADSPAVNGATG-70	<i>Felis catus</i> (cat)
	49-SAINGNPAWHPADSPAVNGATG-70	<i>Oryctolagus cuniculus</i> (rabbit)
	49-SAINGNPSWHLADSPAVNGATG-70	<i>Ovis aries</i> (sheep)
	49-SAINGNPSWHLADSPAVNGATG-70	<i>Sus scrofa</i> (pig)
	49-SAINGNPSWHLADSPANGATG-70	<i>Lemur catta</i> (lemur)
	49-SAINGNPAWHLADSPAVNGATG-70	<i>Saimiri boliviensis</i> (squirrel monkey)
	49-SAINGNPSWHLADSPVVNGATG-70	<i>Callithrix jacchus</i> (new world monkey)
	49-SAINGNPSWHLVDSPAVNGATG-70	<i>Macaca mulatta</i> (old world monkey)
	49-SAINGNPSWHLADSPAVNGATG-70	<i>Pongo abelii</i> (orangutan)
	49-SAINGNPSWHLADSPAVNGATG-70	<i>Homo sapiens</i> (human)

Figure 1. Asparagine-glycine sequences are present in a flexible region between the BH4 and BH3 domains of Bcl-x_L-like proteins from a wide range of species. (A) Schematic demonstrating the relationship between the four Bcl-2 homology (BH) domains, the transmembrane domain (TM), and the conformationally flexible region (curved line) that lies between the BH4 and BH3 domains of human Bcl-x_L. (B) A comparison of the sequences between the BH4 and BH3 domains of Bcl-x_L-like proteins. The sequence surrounding the asparagine-glycine sequence (bolded) in each of these proteins is predicted to be flexible when analyzed by PSIPRED/JPred[27,28]. Genbank accession numbers for these proteins are listed in Table S1.

doi:10.1371/journal.pbio.1001588.g001

develop—that is, deamidation does not occur, if the susceptible asparagines are mutated to alanines to block deamidation. Conversely, Bcl-x_L in which these asparagines are mutated to aspartates to mimic deamidation migrates at the same rate as the more slowly migrating, deamidated forms of wild-type Bcl-x_L[16]. Additionally, deamidation, and therefore, the development of the more slowly migrating forms, can be further induced by incubating Bcl-x_L at an alkaline pH in vitro[16].

We assessed the asparagine-glycine sequences in the flexible loops of Bcl-x_L from *Xenopus laevis* (*Xenopus* Bcl-x_L) and zebrafish for deamidation using the approach outlined above. Wild-type *Xenopus* Bcl-x_L, which contains a single asparagine-glycine sequence in its flexible loop (Figure 3A), forms a doublet when it is expressed in mammalian cells and evaluated by SDS-PAGE (Figure 3B), but only the upper band forms during SDS-PAGE when the cell extract containing the wild-type *Xenopus* Bcl-x_L is first incubated at an alkaline pH (Figure 3B); wild-type zebrafish Bcl-x_L, which contains three asparagine-glycine sequences in its flexible loop (Figure 3A), forms multiple bands (Figure 3B), and there is a relative decrease in the most rapidly migrating band with a concomitant increase in the more slowly migrating bands when it is incubated at an alkaline pH (Figure 3B). Mutation of the

asparagines of the asparagine-glycine sequences to alanines to block deamidation in *Xenopus* Bcl-x_L and zebrafish Bcl-x_L [*Xenopus* Bcl-x_L(N37A) and zebrafish Bcl-x_L(3N/3A), respectively] blocks the formation of the more slowly migrating bands (Figure 3B); mutation of the asparagines to aspartates to mimic deamidation yields forms of Bcl-x_L [*Xenopus* Bcl-x_L(N37D) and zebrafish Bcl-x_L(3N/3D), respectively] that migrate with the upper bands of their respective wild-type proteins (Figure 3B). Finally, the mutant forms of *Xenopus* and zebrafish Bcl-x_L are unaffected when incubated in an alkaline buffer (Figure 3B) (we note that there is a protein band that is most readily visualized in the lanes of the two mutant forms of zebrafish Bcl-x_L that migrates at an intermediate rate and appears to be unaffected by incubation in an alkaline buffer—the nature of this band is unknown). These findings demonstrate that the human, *Xenopus laevis*, and zebrafish forms of Bcl-x_L all have the potential to undergo deamidation.

That deamidation could occur at asparagine-glycine sequences in flexible loops with such disparate sequences as those in human, *Xenopus laevis*, and zebrafish Bcl-x_L-like proteins is consistent with the finding that asparagines that are followed by glycines in flexible regions of proteins are exquisitely labile to deamidation [25,33] and the finding in model peptides that the deamidation rate is

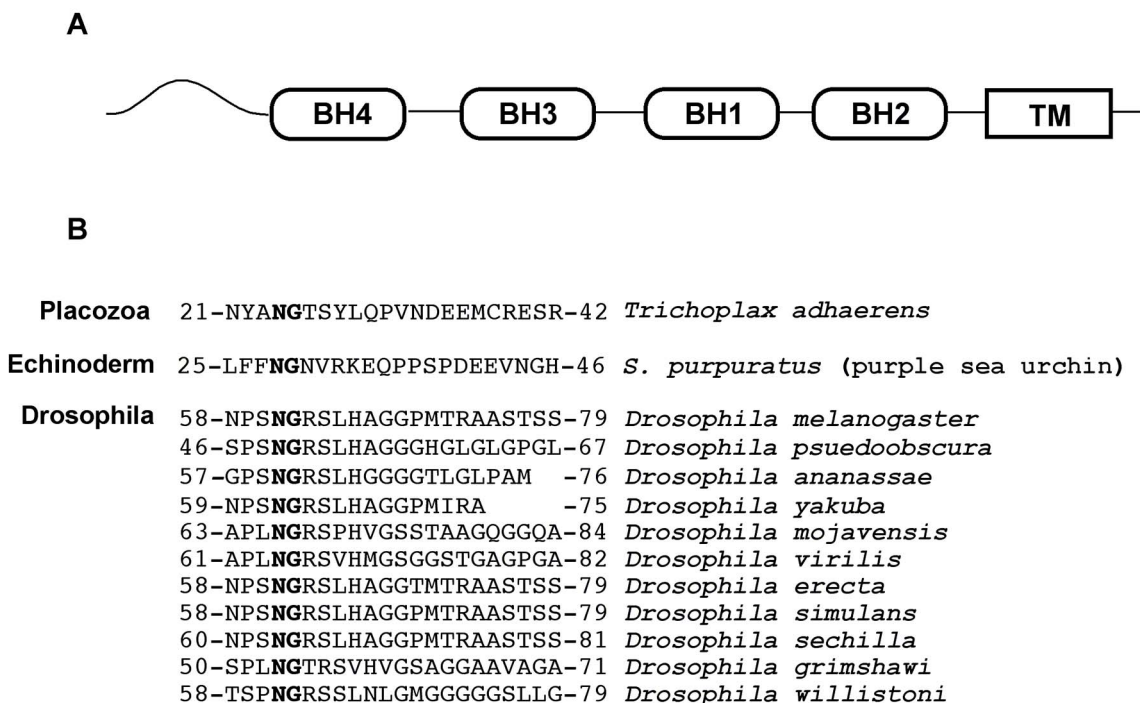


Figure 2. Asparagine-glycine sequences are present in a flexible region that is upstream of the BH4 domain of the Bcl-x_L-like proteins in several species. (A) Schematic demonstrating the position of a unique region (curved line) upstream of the BH4 domain that is predicted to be flexible when analyzed by PSIPRED/JPred [27,28] that is present in the Bcl-x_L-like proteins of several species. (B) Each of these proteins contains an asparagine-glycine sequence (bolded) in the flexible region. Genbank accession numbers for these proteins are listed in Table S1.

doi:10.1371/journal.pbio.1001588.g002

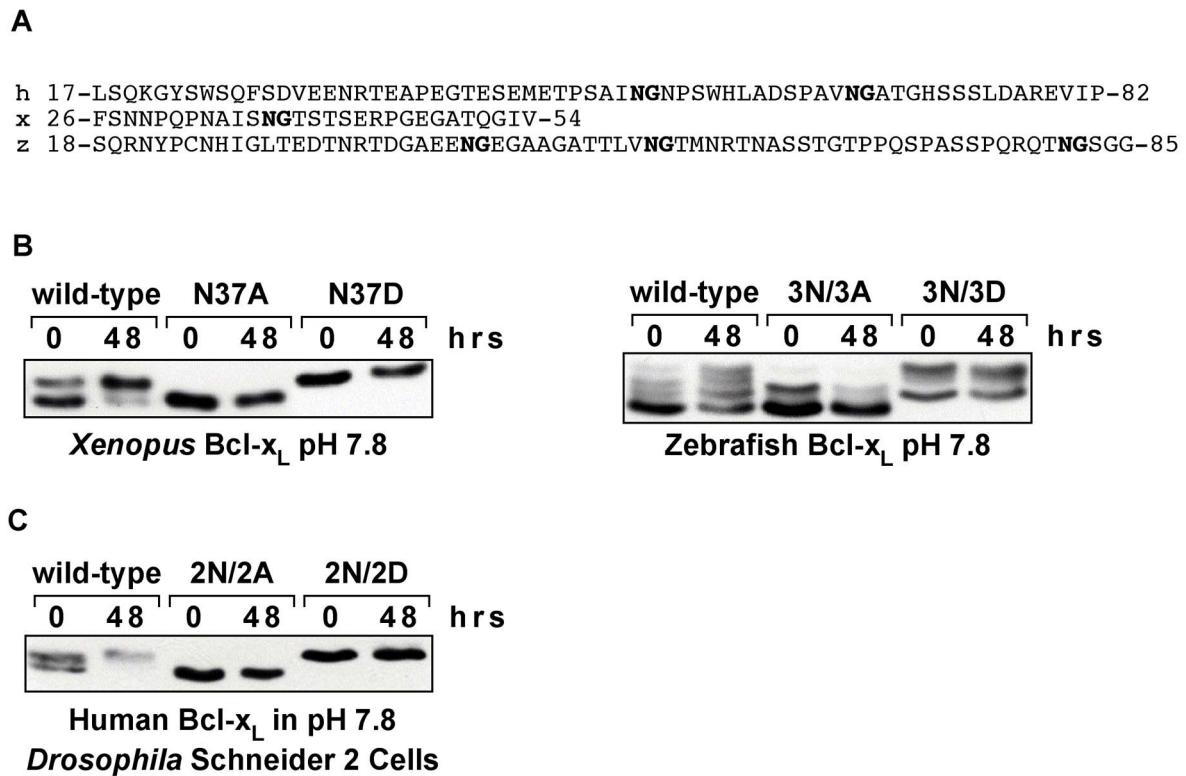


Figure 3. Deamidation is conserved in Bcl-x_L-like proteins. (A) Sequences from the flexible loops of human (h), *Xenopus laevis* (x), and zebrafish (z) Bcl-x_L. Asparagine-glycine sequences are bolded. (B) Anti-HSV immunoblots of HSV-tagged wild-type *Xenopus* and zebrafish Bcl-x_L and mutant forms of *Xenopus* and zebrafish Bcl-x_L in which the asparagines of the asparagine-glycine dipeptides in the flexible loop of each protein are substituted with the indicated amino acids. We have previously demonstrated that the most rapidly migrating form of human Bcl-x_L during SDS-PAGE is the native form and the forms that migrate more slowly are deamidated at one or both sites [16]. *Xenopus* Bcl-x_L was expressed in SAOS-2 cells and zebrafish Bcl-x_L was expressed in C33a cells and lysates of the cells were incubated in a pH 7.8 buffer for the number of hours indicated. Similar results were obtained when *Xenopus* Bcl-x_L was expressed in C33a cells and zebrafish Bcl-x_L was expressed in SAOS-2 cells. (C) Anti-HA immunoblots of HA-tagged wild-type human Bcl-x_L, human Bcl-x_L(N52A/N66A), and human Bcl-x_L(N52D/N66D). Human Bcl-x_L was expressed in *Drosophila* Schneider 2 cells and lysates of the cells were incubated in a pH 7.8 buffer for the number of hours indicated.
doi:10.1371/journal.pbio.1001588.g003

determined primarily by the amino acid that immediately follows the asparagine with the amino acids in surrounding positions having little or no effect [33]. When considered in this context, our findings suggest that deamidation could occur at the asparagine-glycine sequences in the flexible loops of Bcl-x_L-like proteins irrespective of the immediate surrounding sequence. Therefore, our findings suggest that deamidation is a feature of the flexible loop of Bcl-x_L-like proteins across a wide range of species.

We next wanted to determine if Bcl-x_L deamidation occurs in nonmammalian cells. When expressed in *Drosophila* Schneider 2 cells and analyzed by SDS-PAGE, we found that wild-type human Bcl-x_L forms a doublet (Figure 3C). The lower band of the doublet migrated with a mutant form of human Bcl-x_L in which the deamidation is blocked by replacement of the asparagines with alanines [Bcl-x_L(N52A/N66A)] [16], while the upper band of the doublet migrated with a mutant human Bcl-x_L construct in which the susceptible asparagines are replaced with aspartates to generate a constitutively deamidated form of Bcl-x_L [Bcl-x_L(N52D/N66D)] (Figure 3C) [16]. Additionally, when the *Drosophila* Schneider 2 cell lysates were incubated at an alkaline pH prior to SDS-PAGE, the wild-type Bcl-x_L migrated in the position of the upper band of the doublet, while the mutant forms were unaffected (Figure 3C). These findings suggest that the lower band of the doublet found in intact *Drosophila* Schneider 2 cells is

the native form of human Bcl-x_L and the upper band of the doublet is deamidated Bcl-x_L. That Bcl-x_L deamidation occurs in both insect and human cells strongly suggests that deamidation of Bcl-x_L-like proteins can occur in a wide range of species.

Deamidation Targets Human Bcl-x_L for Degradation

The rate of Bcl-x_L deamidation is increased in response to treatment with DNA-damaging agents, such as cisplatin, etoposide, and γ -radiation, in several types of tumor cells [16]. We and others have found that a form of Bcl-x_L in which deamidation is blocked affords tumor cells increased resistance to these agents when compared to the effect of wild-type Bcl-x_L [16,23,24]. Additionally, Zhao and coworkers found that the suppression of Bcl-x_L deamidation by an oncogenic tyrosine kinase contributes to etoposide and γ -radiation resistance in a mouse tumor model [23] and in human myeloproliferative disorders [34], and there is evidence that suppression of Bcl-x_L deamidation is a component of hepatocellular carcinogenesis [35]. These findings suggested that deamidation decreases cellular Bcl-x_L prosurvival activity.

We originally reported that deamidation decreases the prosurvival activity of Bcl-x_L by disrupting its ability to sequester prodeath Bcl-2 family members such as Bim in vivo [16]; however, we subsequently found that our conclusion was based on artifactual results (please see erratum, reference [36]). Surprisingly,

though, another group has since published that deamidation does indeed disrupt the ability of Bcl-x_L to sequester Bim both in vivo and when in solution in vitro [23,37]. Their in vitro findings were particularly surprising because (i) the deamidation sites are positioned near the center of the large unstructured region of Bcl-x_L; (ii) the unstructured region is not necessary for the interaction with Bim or for the antiapoptotic activity of Bcl-x_L [38]; (iii) the unstructured region remains unstructured in the deamidated form of Bcl-x_L [39]; and (iv) the native and deamidated forms of Bcl-x_L “adopt an essentially identical backbone structure” in solution [39]. Therefore, we reexamined the effect of deamidation on the ability of Bcl-x_L to bind Bim using several different approaches and controls. We found that deamidation has no effect on the ability of Bcl-x_L to bind Bim or Bax (Text S1 and Figure S2). This is consistent with the finding that both the native and deamidated forms of Bcl-x_L bind equally to PGAM5, a protein that has been implicated in oxidative stress-induced apoptosis [40]. Furthermore, Bcl-x_L encodes several additional presumed prosurvival activities, such as the ability to bind to p53 [41–43] and the ability to regulate mitochondrial membrane permeability by forming an ion channel [44–46]. It seemed unlikely that deamidation within the unstructured loop could directly inactivate all of these functions. Therefore, we sought the mechanism by which deamidation decreases cellular Bcl-x_L prosurvival activity.

We noted that the levels of endogenous Bcl-x_L decreased as deamidation increased in several of our previous experiments (e.g., figure 2 and figure 6 in reference [16]) and a correlation between deamidation and decreased Bcl-x_L levels in maturing erythrocytes was noted by Koury and coworkers [47]. Furthermore, in cells in which apoptosis was induced by oxidative damage, a fragment of Bcl-x_L, but not full-length Bcl-x_L, was found to be bound to an enzyme that binds deamidated proteins [48], which suggests that Bcl-x_L is rapidly degraded upon deamidation. Therefore, we considered the possibility that deamidation decreases the cellular activities of Bcl-x_L by targeting Bcl-x_L for degradation. Indeed, we found a clear correlation between the DNA damage-induced increase in Bcl-x_L deamidation and a decrease in Bcl-x_L levels (Figure 4A).

To begin to determine if it is specifically the deamidated forms that are targeted for degradation, we first blocked synthesis of the native form of Bcl-x_L using cycloheximide. We found that the level of the native Bcl-x_L decreases first and then, once the native Bcl-x_L is depleted, the level of deamidated Bcl-x_L decreases (Figure 4B). The simplest explanation for this finding is that the native Bcl-x_L is constantly deamidated, even in cells that have not been treated with DNA damaging agents, and the deamidated forms are degraded.

To confirm that the deamidated forms are specifically targeted for degradation, we compared the stability of wild-type Bcl-x_L and a form of Bcl-x_L in which deamidation is blocked because the susceptible asparagines are mutated to alanines, [Bcl-x_L(N52A/N66A)] [16]. We have previously shown that the signaling that increases the rate of Bcl-x_L deamidation in cells that are treated with DNA damaging agents is suppressed in wild-type mouse embryo fibroblasts (MEFs) and that the suppression is dependent upon the activation of pRb by p53 signaling [16]. Therefore, to determine if deamidation targets Bcl-x_L for degradation we reconstituted Bcl-x_L expression in *bcl-x*^{-/-}/*p53*^{-/-} MEFs with either wild-type Bcl-x_L or Bcl-x_L(N52A/N66A). Importantly, we expressed each protein using retroviral infection at a multiplicity of infection of <1 without polybrene treatment or centrifugation so that instead of overexpressing the Bcl-x_L constructs at high levels, we approximated the level of Bcl-x_L found in wild-type MEFs as

closely as possible. After antibiotic selection for the infected cells, we treated the pooled cells with etoposide or cisplatin to induce increased deamidation of Bcl-x_L. Whereas the level of wild-type Bcl-x_L decreased progressively after etoposide or cisplatin treatment, the level of Bcl-x_L(N52A/N66A), the form of Bcl-x_L in which deamidation is blocked, remained relatively constant (Figure 4C). As would be expected, the cells expressing Bcl-x_L(N52A/N66A) were more resistant to the apoptotic effects of etoposide and cisplatin than were the cells in which the wild-type Bcl-x_L was expressed (Figure 4D). These findings strongly suggest that deamidation mediates the inactivation of Bcl-x_L prosurvival activity by mediating the degradation of Bcl-x_L.

Proteins that are subject to regulatory degradation often contain PEST sequences and the presence of PEST sequences is specific to such proteins—that is, PEST sequences are rarely found in long-lived cellular proteins[49]. PEST sequences are hydrophilic stretches of at least 12 amino acids that are enriched in prolines, glutamates, aspartates, serines, and threonines that are flanked by but do not contain histidines, arginines, or lysines [50]. The PESTfind algorithm identifies potential PEST sequences and assigns them a score that predicts the likelihood that they truly function as a degradation signal sequence [50]. A score above zero denotes a potential PEST sequence[50]; the higher the score, the more likely the sequence functions to target the protein for degradation. Whereas the most well characterized PEST sequence, the PEST sequence in IκBα, has a PESTfind score of 5.90[49], human Bcl-x_L contains a PEST sequence with a score of 10.79, which suggested that we would find that the human Bcl-x_L PEST sequence truly functions as a proteolytic signaling sequence. It is also notable that (i) the PEST sequence is conserved among all mammalian forms of Bcl-x_L (Figure 5); (ii) even though the sequences themselves differ considerably from the mammalian sequence, there are sequences that are identified by the PESTfind algorithm as potential PEST sequences in a similar position in the Bcl-x_L-like proteins from a wide range of nonmammalian species (Figure 5)—that is, suggesting that there is conservation of a specific function at this position even though the sequence is not conserved; and (iii) PEST sequences only occur infrequently and indeed, there are no other sequences with PESTfind scores greater than zero at any other position within any of the Bcl-x_L-like proteins listed in Figure 1B. These findings argue strongly for the importance of a functional PEST sequence at this position.

Importantly, a PEST sequence may either constitutively or conditionally target a protein for proteolysis [49]. Therefore, it was intriguing that the PEST sequences either encompass or are in close proximity to the deamidation sites (Figure 5). This was intriguing because phosphorylation within or in proximity to certain conditional PEST sequences increases proteolytic signaling [49] and the products of deamidation, aspartyl residues, can functionally mimic phosphorylated amino acids [51]. Similarly, because deamidation adds an aspartyl residue, it increases the hydrophilicity and, hence, the PESTfind score of the PEST sequence (e.g., the PESTfind score of human Bcl-x_L increases from 10.79 to 13.40 upon deamidation), which suggested that deamidation increases the activity of the PEST sequence. Therefore, we assessed the possibility that, like phosphorylation in other proteins, deamidation activates the PEST sequence as a signal for the proteolysis of Bcl-x_L.

To test this, we generated a human Bcl-x_L construct in which the three prolines of the PEST sequence are mutated to alanines [Bcl-x_L(3P/3A)] to partially disrupt its activity. We found that the level of deamidated Bcl-x_L(3P/3A) relative to the native form is increased when compared with wild-type Bcl-x_L in untreated cells

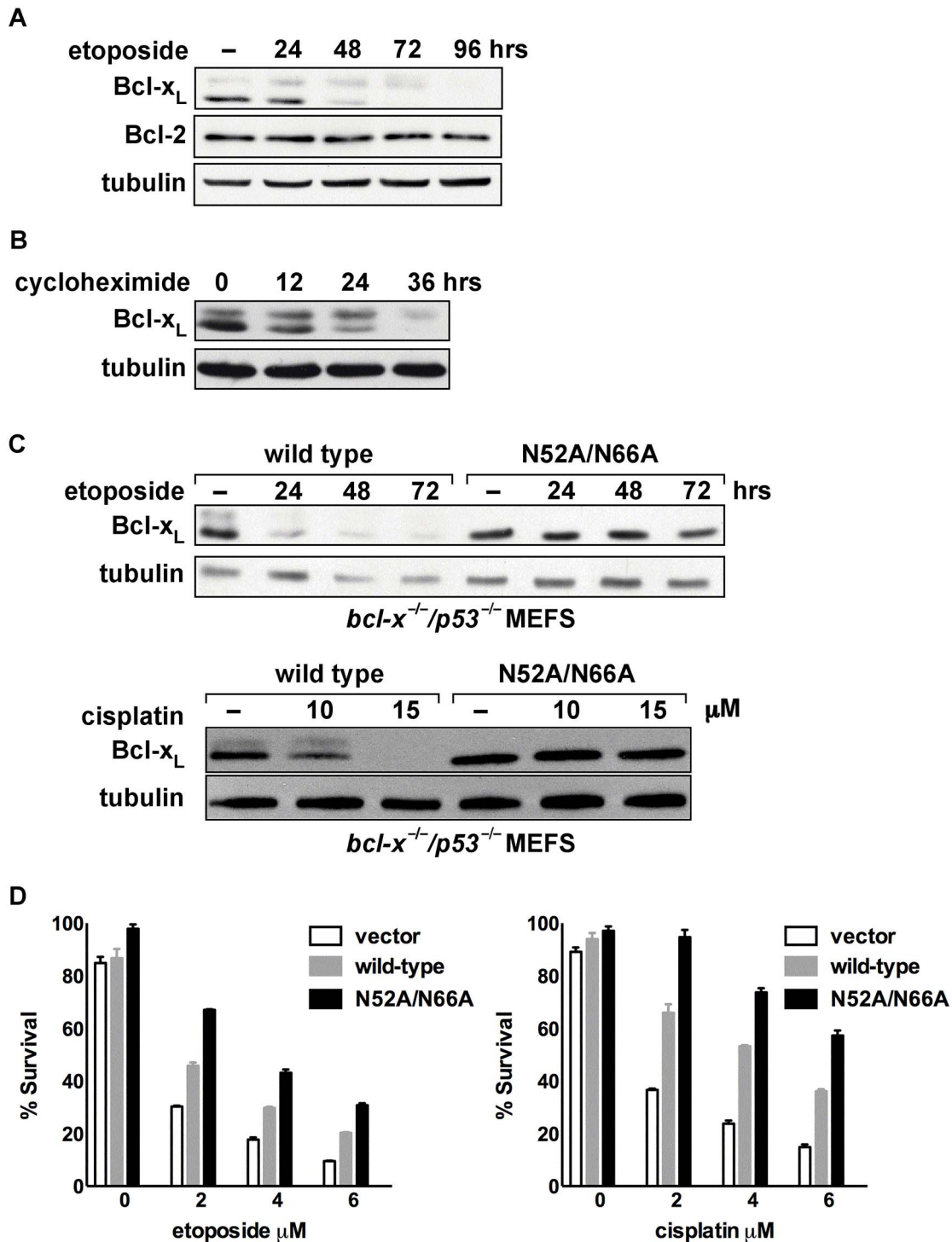


Figure 4. Deamidation targets Bcl-x_L for degradation. (A) Immunoblot of endogenous Bcl-x_L, Bcl-2, and tubulin from SAOS-2 cells that were treated with 10 μM of etoposide for the indicated times. (B) Immunoblot of endogenous Bcl-x_L and tubulin in SAOS-2 cells that were treated with 10 μg/ml of cycloheximide for the indicated times. (C) Immunoblot of Bcl-x_L and tubulin in *bcl-x^{-/-}/p53^{-/-}* MEFs expressing wild-type Bcl-x_L and a form of Bcl-x_L in which deamidation is disrupted by substitution of alanines for the two susceptible asparagines, Bcl-x_L(N52A/N66A). The cells were treated with 5 μM of etoposide for the indicated times or with the indicated concentration of cisplatin. (D) Survival assays of *bcl-x^{-/-}/p53^{-/-}* MEFs expressing Bcl-x_L(N52A/N66A) and wild-type Bcl-x_L. MEFs were treated with etoposide and cisplatin and assessed for apoptosis after 72 h. doi:10.1371/journal.pbio.1001588.g004

and cells treated with etoposide (Figure 6A) and that this is due to increased stability of the deamidated forms (Figure 6B). Furthermore, the cells expressing Bcl-x_L(3P/3A) were significantly more

resistant to etoposide- and cisplatin-induced apoptosis than those expressing wild-type Bcl-x_L (Figure 6C). The simplest explanation for these findings is that the function of Bcl-x_L deamidation is to

Fish	pufferfish	28-SRTEGQFGTTQ NGTFNG ASPGTTPPAPSOHQOQSLTSL-64	(7.90)
	cod	28-YRPIPFQPEGAGEGTD EDKSNRIGNNG- LRLNDG NGNG QLAPSPTPOGTEAVRA	(7.03) -80 (1.61)
Amphibian	<i>X. laevis</i>	24-RKFSNNPQPN AI NGTSTSERPGEGATQGI V EEVLQ-60	(3.30)
Reptile	turtle	12-IRTESAEEAEMASVP NG SPSWHPGASHVV NGA AAGHSN-48	(9.29)
	anole	24-WHEIEMESGEEAMEPANETGNTL NG SPSWHPPSPSHVI-60	(9.38)
Bird	striated finch	33-NRTDFAGEEDEM DGVLNG SPSWHAATSHIV NGAT VHQ-69	(5.07)
	zebra finch	33-NRTDFAGEEDEM DGVLNG SPSWHAATSHIV NGAT VHQ-69	(5.07)
	willow grouse	26-NRTDTAAEAEMDSVL NG SPSWHPPAGHV NGAT VHRS-62	(4.41)
	chicken	33-NRTDTAAEAEMDSVL NG SPSWHPPAGHV NGAT VHRS-69	(4.41)
	turkey	33-NRTDTAAEAEMDSVL NG SPSWHPPAGHV NGA AVHRS-69	(4.41)
Mammal	opossum	31-NRTEVLEGAEIPSTV NG SPSWHPADSRAVSGATGHSS-67	(2.89)
	dunnart	31-NRTEAPEGTELPSTV NG SPSWHPADSRAGSGATGHSS-67	(11.65)
	hamster	33-NRTEAPEGTESE RE TPSA ING NPSWHLADSPAV NGAT -69	(18.28)
	ground squirrel	13-NRTEAPEGTESE VE TPSA ING NPSWQLADSPA INGAT - GHSSLDAREVIPMAAVKQAL	(9.81) -70
	cow	33-NRTEAPEGTESE DM ETPSA ING NASWHLADSPAV NGAT -69	(10.73)
	rabbit	33-NRTEAPEGTGPE ME TPSA ING NP A WHPADSPAV NGAT -69	(8.55)
	sheep	33-NRTEAPEGTESE DM ETPSA ING NPSWHLADSPAV NGAT -69	(13.18)
	pig	33-NRTEAPEGTESE AE TPSA ING NPSWHLADSPAV NGAT -69	(14.57)
	lemur	33-NRTEAPEGTESE ME TPSA ING NPSWHLADSP P AV NGAT -69	(13.40)
	squirrel monkey	33-NRTEAPEGTDSE ME TPSA ING NP A WHLADSPAV NGAT -69	(10.98)
	new world monkey	33-NRTEAPEGTDSE ME TPSA ING NPSWHLADSP VV AV NGAT -69	(13.18)
	human	33-NRTEAPEGTESE ME TPSA ING NPSWHLADSPAV NGAT -69	(13.40)

Figure 5. The PEST sequence is conserved among a wide range of nonmammalian and all mammalian forms of Bcl-x_L. PEST sequences are underlined and asparagine-glycine sequences are bolded. PESTfind scores[78] were calculated for the deamidated form of each protein. Representative mammalian PEST sequences are shown; all of the mammalian forms of Bcl-x_L that are listed in Figure 1B contain PEST sequences that are either identical to or near identical to these sequences.
doi:10.1371/journal.pbio.1001588.g005

increase the proteolytic targeting activity of the Bcl-x_L PEST sequence.

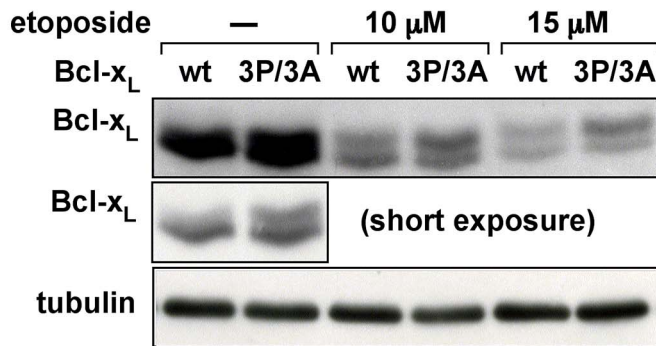
Importantly, in the experiment depicted in Figure 6A and in several of the experiments discussed below, the Bcl-x_L constructs are overexpressed and they therefore prevent induction of the later phases of apoptosis. However, even the overexpressed Bcl-x_L undergoes an increase in deamidation-regulated degradation upon treatment with DNA-damaging agent agents. This indicates that deamidation-regulated degradation of Bcl-x_L is a function of changes that occur in the cell during the premitochondrial phase of apoptosis, the phase in which decreases in Bcl-x_L would increase susceptibility to prodeath signaling. This finding and the conservation of the PEST sequence together provide strong evidence of the functional significance of the deamidation-regulated degradation of Bcl-x_L as an integral component of the rheostat that regulates cell death.

Bcl-x_L is cleaved by calpain both in vitro and in vivo [52–54], which is notable because PEST sequences can target proteins for calpain-mediated degradation [55–57]. Therefore, to begin to identify the protease(s) that mediate degradation of deamidated Bcl-x_L, we treated HTB-9 and C33a cells with calpain inhibitor I and found that it causes primarily an increase of deamidated Bcl-x_L in both (Figure 7A). Additionally, the deamidated forms of Bcl-x_L are increased by calpain inhibitor I when Bcl-x_L deamidation is

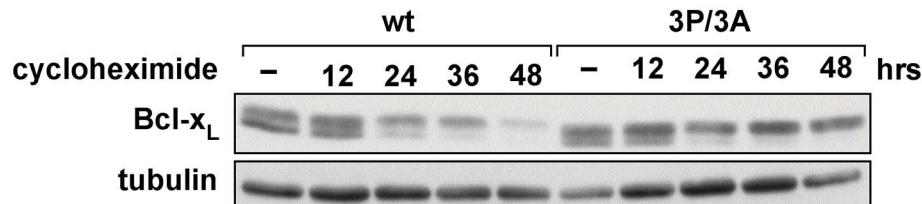
further induced by etoposide treatment (Figure 7B). Importantly, the increase in the deamidated forms in the cells treated with calpain inhibitor I is due to an increase in stability as assessed by a pulse chase experiment (Figure 7C), demonstrating that calpain inhibitor I increases Bcl-x_L levels by blocking its degradation.

Importantly, calpain inhibitor I inhibits several different proteases, not just calpain. In fact, calpain inhibitor I also inhibits the proteasome, albeit at a higher concentration than that which is required to inhibit calpain, and PEST sequences can target proteins for proteasomal degradation. We therefore assessed a known proteasomal target, Mcl-1, on the same blot in which we had examined the effect of calpain inhibitor I on Bcl-x_L in HTB-9 cells. We also examined total cellular ubiquitinated proteins in the same cell lysates. Whereas 5 μM calpain inhibitor I had caused a near maximal increase in the level of the deamidated forms of Bcl-x_L (Figure 7A), Mcl-1 and total ubiquitinated proteins only reached near maximal levels when the cells were treated with 15–20 μM calpain inhibitor I (Figure 7D). We also found that the specific proteasome inhibitor lactacystin had only a relatively small, if any, effect on Bcl-x_L compared with its effect on MCL-1 and total ubiquitinated proteins in HTB-9 cells (Figure 7E). These findings suggest that the proteasomal activity does not have a significant role in the degradation of the deamidated form of Bcl-x_L.

A



B



C

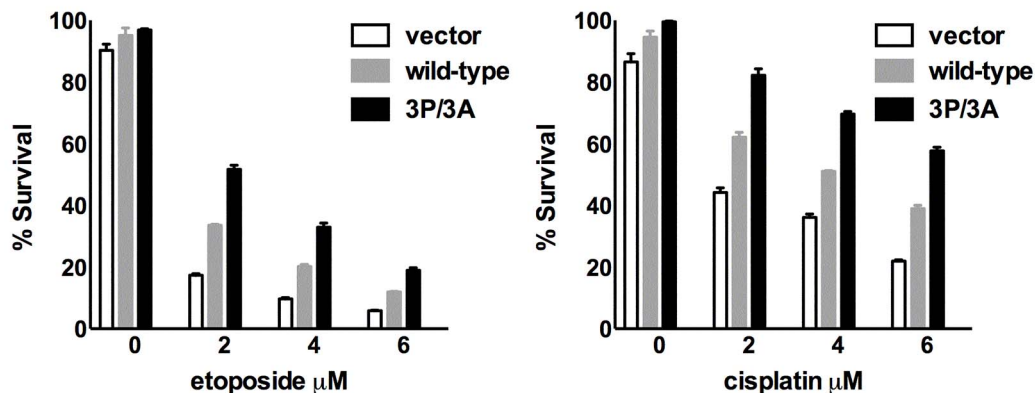


Figure 6. Deamidation activates a conditional PEST sequence to target Bcl-x_L for degradation. (A) Immunoblot of Bcl-x_L in *bcl-x*^{-/-}/*p53*^{-/-} MEFs infected with vectors for wild-type Bcl-x_L or a form of Bcl-x_L in which the PEST sequence is disrupted by substitution of alanines for three of the PEST sequence prolines, Bcl-x_L(3P/3A), that were treated with etoposide as indicated. Two different exposures of the immunoblot are shown to facilitate the visualization of deamidated forms of Bcl-x_L. (B) Anti-HA and tubulin immunoblot of 2 μg/ml of cycloheximide-treated SAOS-2 cells expressing HA-tagged versions of wild-type Bcl-x_L or Bcl-x_L(3P/3A) for the indicated times. (C) Survival assay of *bcl-x*^{-/-}/*p53*^{-/-} MEFs expressing Bcl-x_L(3P/3A) and wild-type Bcl-x_L. MEFs were treated with etoposide or cisplatin as indicated and survival was assessed at 48 h. doi:10.1371/journal.pbio.1001588.g006

Bcl-x_L has also been shown to be degraded by caspases [58]. However, we found that stable expression of a dominant negative form of caspase 9 had no effect on Bcl-x_L degradation in response to etoposide treatment in SAOS-2 cells even though the dominant negative caspase 9 blocked activation of caspase 3 (Figure 7F) and apoptosis (unpublished data). Expression of the retinoblastoma protein (pRb), which blocks Bcl-x_L deamidation [16], was used as

a control (Figure 7F). That expression of the dominant negative caspase 9 fails to block degradation of deamidated Bcl-x_L is consistent with the finding that overexpressed Bcl-x_L is degraded even though its overexpression should block caspase activation. Together these findings demonstrate that caspase activity is not necessary for DNA damage-induced Bcl-x_L degradation, at least in certain cell lines.

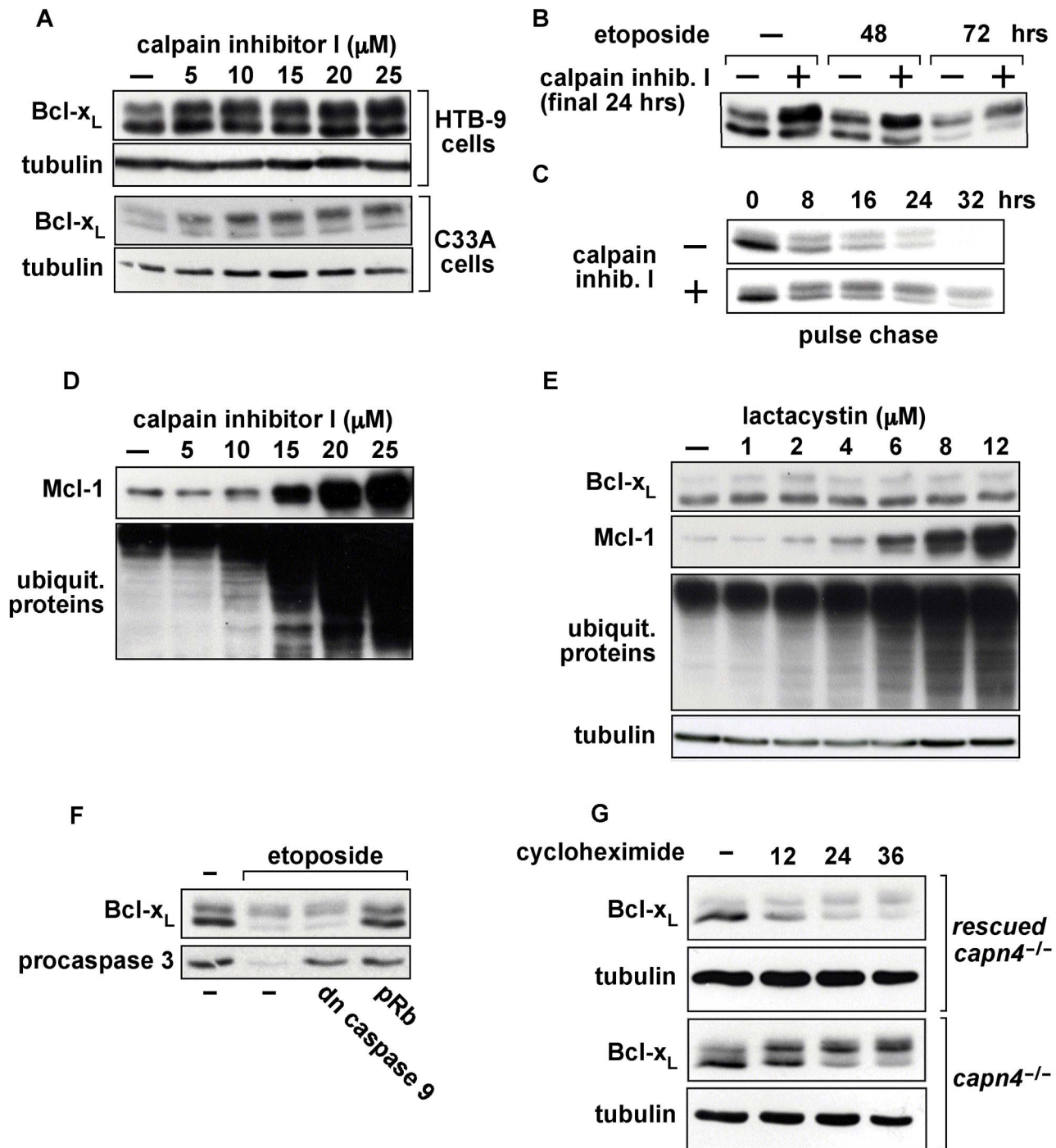


Figure 7. Deamidated Bcl-x_L is degraded by calpain. (A) Immunoblots of endogenous Bcl-x_L and tubulin in HTB-9 and C33a cells that were treated with calpain inhibitor I for 24 h. (B) Immunoblot of endogenous Bcl-x_L from HTB-9 cells that were treated with 10 μM of etoposide for the indicated times and with 10 μM of calpain inhibitor I for the final 24 h of the etoposide treatment. (C) Pulse chase of overexpressed Bcl-x_L in Bcl-x_L-inducible SAOS-2 cells that were treated with 10 μM of calpain inhibitor I as indicated. The contrast of this figure was increased to facilitate visualization of the data. (D) The HTB-9 blot from Figure 7A was reprobed for Mcl-1 and the same lysates that were used for the HTB-9 blot in Figure 7A were probed for total ubiquitinated proteins. (E) Immunoblot of endogenous Bcl-x_L, Mcl-1, and total ubiquitinated proteins from HTB-9 cells that were treated with the lactacystin for 24 h. Mcl-1 and total ubiquitinated proteins were used as positive controls to evaluate proteasomal activity. (F) Immunoblots of Bcl-x_L and procaspase 3 from etoposide-treated SAOS-2 cells in which a dominant negative form of caspase 9 or pRb was expressed. (G) Anti-Bcl-x_L immunoblot of *Capn4*^{-/-} MEFs that were rescued by expression of *Capn4* and *Capn4*^{-/-} MEFs that were treated with cycloheximide for the indicated times. Tubulin was used as a loading control.
doi:10.1371/journal.pbio.1001588.g007

Finally, to further examine the potential role of calpain in the degradation of deamidated Bcl-x_L, we examined Bcl-x_L in fibroblasts that lack calpain activity [59]. The *Capn4* gene encodes the small subunit of calpain, which is necessary for all calpain activity. When *Capn4*^{-/-} MEFs in which calpain activity was rescued by expression of the *Capn4* gene were treated with cycloheximide, Bcl-x_L decreased (Figure 7G), as it does in other cells that have calpain activity when they are treated with cycloheximide (e.g., Figures 4B and 6B). However, Bcl-x_L accumulated in its deamidated form in *Capn4*^{-/-} MEFs when they were treated with cycloheximide. These findings are consistent with a role for calpain in the degradation of deamidated Bcl-x_L.

Regulation of Bcl-x_L Deamidation by Changes in Cellular pH

It is widely accepted that there is a rapid fall in cytosolic pH of ≈0.3–0.4 units that occurs in apoptosis upon mitochondrial outer membrane permeabilization [60,61]; however, several groups have reported that cytosolic alkalinization to as high as pH 8.0 occurs early in certain forms of apoptosis, including DNA damage-induced apoptosis [62–67]. This is notable because based on structural considerations, Bcl-x_L is predicted to be exquisitely susceptible to nonenzymatic deamidation at pH 7.4 [16,68] and it has been demonstrated that the rate of Bcl-x_L deamidation in reticulocyte lysates is increased significantly by increases in pH within the range of pH 7.0 to pH 8.0 [47]. These findings strongly suggested that DNA damage-induced Bcl-x_L deamidation is regulated by changes in pH in the cell. Indeed, while this work was in progress, it was confirmed that the DNA damage-induced increase in Bcl-x_L deamidation in lymphocytes is induced by the increase in cytosolic pH that occurs in response to DNA damage [37] and we have confirmed that this is also true in the cells of human solid tumors (Text S2 and Figure S3). Notably, the finding that the rate of deamidation is increased by increased pH is further evidence that the DNA damage-induced increase in deamidation of Bcl-x_L occurs in the premitochondrial phase of apoptosis, because, as noted above, the onset of the postmitochondrial phase is characterized by a rapid acidification of the cytosol [60,61], which would be expected to decrease the rate of deamidation of Bcl-x_L.

We previously reported that expression of pRb in SAOS-2 osteosarcoma cells blocks both the DNA damage-induced increase in Bcl-x_L deamidation and apoptosis [16]. Indeed, we now report that expression of pRb decreases pH in these cells at baseline and after treatment with DNA-damaging agents (Figure 8A). This strongly suggests that Rb blocks an increase in the rate of Bcl-x_L deamidation by maintaining the cytoplasm at a relatively low pH after treatment with DNA-damaging agents. This is notable because we found that inhibition of Bcl-x_L expression renders SAOS-2 cells that express pRb susceptible to DNA damage-induced apoptosis [16]. Together these findings strongly suggest that the increased rate of deamidation-regulated degradation of Bcl-x_L is an important function of the increase in pH that occurs in response to treatment with DNA-damaging agents—that is, alkalinization is necessary to induce an increased rate of deamidation-regulated degradation of Bcl-x_L, which in turn is necessary for apoptosis to occur, but alkalinization is not necessary if Bcl-x_L is absent.

We have also reported that the DNA damage-induced increase in Bcl-x_L deamidation is suppressed in wild-type MEFs, but it occurs in *p53*^{-/-} MEFs. This is notable because while pRb is activated by DNA damage in wild-type MEFs, it remains inactive after DNA damage occurs in *p53*^{-/-} MEFs [16]. Therefore, we

hypothesized that the activated pRb in the wild-type MEFs suppresses Bcl-x_L deamidation. Consistent with this and our finding that pRb suppresses the alkalinization in SAOS-2 cells, we found that while *p53*^{-/-} MEFs are susceptible to the DNA damage-induced alkalinization, wild-type MEFs are not (Figure 8B). Finally, we found that even though *bcl-x*^{-/-} MEFs, which have an intact p53-pRb signal transduction pathway, are exquisitely susceptible to apoptosis [16], they do not exhibit a DNA damage-induced increase in cytosolic pH prior to undergoing apoptosis (Figure 8C). This last finding is further evidence that the increased rate of deamidation-regulated degradation of Bcl-x_L is an important target of the increase in pH that occurs in response to treatment with DNA-damaging agents in susceptible tumor cells.

Discussion

Asparagine deamidation was long thought to be a purification artifact; however, in 1968 Flatmark provided the first demonstration that a protein undergoes deamidation within the cell [69]. It is now well accepted that many proteins undergo deamidation within the cell, but deamidation is still viewed nearly universally as a form of protein damage or aging that is detrimental to the organism. This is because deamidation has been thought by most to be an unregulated, spontaneous process that disrupts protein function through the nonspecific disruption of protein structure. Furthermore, whereas deamidation has been implicated in the dysfunction underlying several pathologic processes, such as Alzheimer's disease [70] and cataract formation [71], there has been only limited evidence that it could serve a beneficial role [72].

We have now demonstrated that Bcl-x_L deamidation is a process that activates a conditional PEST sequence. The degree of organization underlying both the regulation and functional consequence of Bcl-x_L deamidation together with the fact that it is conserved across a wide range of species clearly suggests that deamidation can play a beneficial regulatory role. It is possible that the deamidation that occurs in Alzheimer's disease, cataract formation, and other pathologic processes represents a dysregulated state of a process that normally has an important cellular function. This would be analogous to the contribution of the dysregulation of the phosphorylation of certain proteins to tumorigenesis [73]. Indeed, there is evidence that the dysregulation of Bcl-x_L deamidation contributes to the development of hepatocellular carcinoma [35] and myeloproliferative disorders [34]. Notably, in addition to pH, the rate of deamidation is affected by the buffer ion, tonicity, and temperature [74]. A change in any of these that results in a decrease in the rate of Bcl-x_L deamidation would have the potential to increase tumor cell viability and inhibit the tumor cell response to treatment, worsening patient outcome.

Additionally, we have shown that even modest changes in Bcl-x_L levels can alter the extent of tissue damage in response to certain types of injury [17]. The finding that mutation of the PEST sequence or treatment with calpain inhibitor I in otherwise untreated cells results in a relative increase of the level of deamidated Bcl-x_L demonstrates that Bcl-x_L levels are continuously modulated by deamidation, even in normally growing cells. Therefore, any change in factors that affects the rate of deamidation could alter the extent of tissue damage in response to certain types of injury.

Finally we note that asparagine deamidation is an extraordinarily simple posttranslational modification in that it only requires a water molecule to proceed. Its simplicity suggests that it was an early form of posttranslational modification. In this context, it is

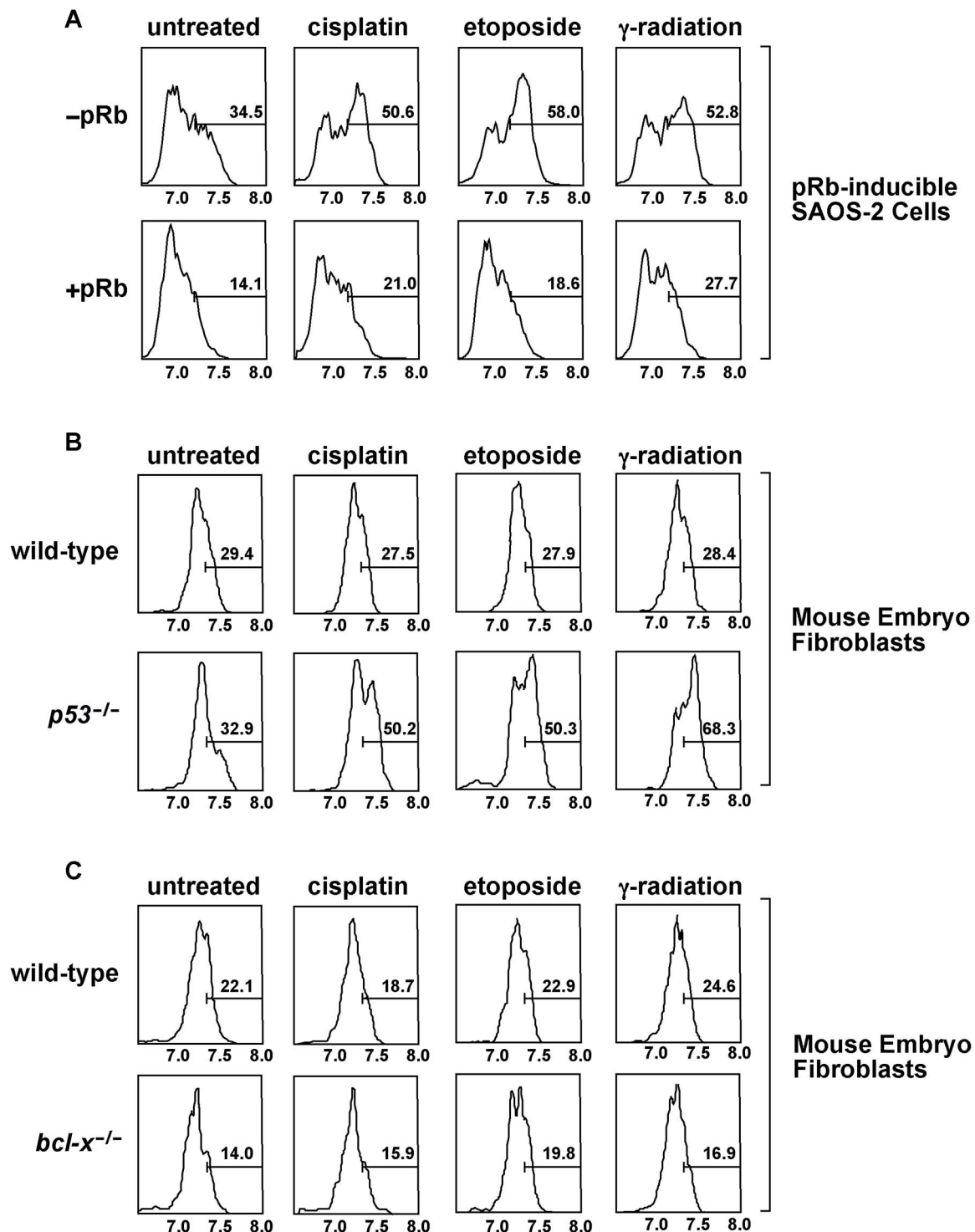


Figure 8. Deamidation-mediated degradation of Bcl-x_L is an important function of the DNA damage-induced increase in cellular pH. (A) Rb-inducible SAOS-2 cells were treated with the indicated DNA-damaging agents. Rb expression was induced by treatment with doxycycline prior to DNA-damaging agent treatment. The percent of adherent cells with a pH above an arbitrarily chosen value of approximately pH 7.3 is indicated. (B) Wild-type and *p53*^{-/-} MEFs were treated with the indicated DNA-damaging agents and the intracellular pH was measured. (C) Wild-type and *bcl-x*^{-/-} MEFs were treated with the indicated DNA-damaging agents and the intracellular pH was measured. doi:10.1371/journal.pbio.1001588.g008

notable that asparagine is the evolutionary offspring of aspartate and it is thought that asparagine “captured” what were originally two aspartate codons to serve as its codons [75]. Thus we speculate

that asparagines replaced certain aspartates as proteins evolved so that a residue with an inducible negative charge, asparagine, could replace a residue with a fixed negative charge, aspartate. This

substitution would have afforded a greater degree of control of protein function. Indeed, it may have been the selective advantage of the potential to switch from a neutral residue to a charged residue that initially drove the stable incorporation of asparagine into proteins.

Materials and Methods

MEME Analysis

The protein sequences listed in the Bcl-x_L (BCL2L1) homology group of the Bcl-2 database (Figure S1) [29] that contain both a BH4 and a BH3 domain were identified using the online Batch Search tool of the Conserved Domain Database [76]. The intervening sequences between the BH4 and BH3 domains in these proteins were compiled to form the dataset that was submitted to the MEME server for analysis. Importantly, there are species in the database that express more than one protein in which the sequence between the BH4 and BH3 domains are identical; such proteins are typically the result of alternative splicing. In such instances, the sequence was only included once in the analysis.

Cell Culture, Plasmids, and Retroviral Constructs

SAOS-2 cells (ATCC HTB-85), C33a cells (ATCC HTB-31), and MEFs were maintained in DMEM with 10% FBS. HTB-9 cells (ATCC HTB-9) were maintained in RPMI-1640 with 10% FBS. *Drosophila* Schneider 2 cells were maintained in Shields and Sang M3 (Sigma) with 10% FBS. *bcl-x*^{-/-}, *p53*^{-/-}, and *bcl-x*^{-/-}/*p53*^{-/-} MEFs and Rb-inducible SAOS-2 cells were described previously [16]. Capn4^{-/-} MEFs were described previously [59]. Bcl-x_L-inducible SAOS-2 cells were generated using the T-Rex system (Invitrogen). *Xenopus* and zebrafish Bcl-x_L cDNAs were amplified by RT-PCR using primers 5'-ATATATCCATGGCAGAGGGCAGCAGTAGAGATCTGGTGG-3' and 5'-TATA-TACAGCTGTCGGCGCCTCATGTAGCAGACC-3' with *Xenopus* mRNA and 5'-ATATATCCTGGCATCTTACTA-TAACCGAGAACTGGTGG-3' and 5'-TATATACAGCTGCAGGCGTTTCTGTGCAATGAGTCCCCC-3' with zebrafish mRNA (the underlined sequences in the primers were used for cloning purposes). The products were cloned between the *Nco* I site and *Pvu* II site in the plasmid pTriEx-1.1 (Novagen). The sequences of the inserts were confirmed as identical to the *Xenopus* Bcl-x_L sequence (Genbank accession no. NP001082147) and the zebrafish Bcl-x_L sequence (Genbank accession no. NP571882) listed in the NCBI databases. All mutations were made using the QuikChange Kit (Stratagene). *Xenopus* Bcl-x_L codon 37 was changed from AAT to GCT to generate *Xenopus* Bcl-x_L(N37A) and codon 37 was changed from AAT to GAT to generate *Xenopus* Bcl-x_L(N37D). Zebrafish Bcl-x_L codon 42 was changed from AAT to GCT, codon 54 from AAT to GCT, and codon 81 from AAT to GCT to generate zebrafish Bcl-x_L(3N/3A), and codon 42 was changed from AAT to GAT, codon 54 from AAT to GAT, and codon 81 from AAT to GAT to generate zebrafish Bcl-x_L(3N/3D). For expression of the wild-type and mutant forms of human Bcl-x_L in *Drosophila* Schneider 2 cells pCMA-Bcl-x_L, pCMA-Bcl-x_L(N52A/N66A), and pCMA-Bcl-x_L(N52D/N66D) were constructed by ligation of PstI Bcl-x_L encoding fragments from pSFFV-Bcl-x_L, pSFFV-Bcl-x_L(N52A/N66A), and pSFFV-Bcl-x_L(N52D/N66D) [16] into the PstI site of pCMA [77]. Retroviral vectors for expression of wild-type and mutant forms of human Bcl-x_L were generated as follows. The retroviral construct pBABE-blast and pBABE-blast-HA were generated by ClaI/HindIII digest of pBABE-puro and pBABE-puro-HA (removes the puromycin resistance gene) and blunt-end ligation of the blasticidin resistance gene with its promoter from pCDNA/TR (Invitrogen) into these

sites. pBABE-blast-Bcl-x_L, pBABE-blast-Bcl-x_L(N52A/N66A), and pBABE-blast-HA-Bcl-x_L were constructed by ligation of the EcoRI Bcl-x_L encoding fragments from pSFFV-Bcl-x_L and pSFFV-Bcl-x_L(N52A/N66A) [16] into the EcoRI site of pBABE-blast and pBABE-blast-HA. In pBABE-blast-Bcl-x_L and pBABE-blast-HA-Bcl-x_L, Bcl-x_L codon 38 was changed from CCA to GCA, codon 48 from CCC to GCC, and codon 55 from CCA to GCA to generate pBABE-blast-Bcl-x_L(3P/3A) and pBABE-blast-HA-Bcl-x_L(3P/3A). pCDNA3-Flag-dominant negative caspase 9 was described previously [16].

Infection and Transfection

Retroviral particles were produced by transient transfection of Phoenix E cells with either pBABE-blast-Bcl-x_L or pBABE-blast-Bcl-x_L(N52A/N66A). The pBABE-blast-Bcl-x_L and pBABE-blast-Bcl-x_L(N52A/N66A) supernatants were collected from the Phoenix E cell cultures and diluted 1:5 in fresh media. The diluted retrovirus was added to the medium of the MEFs without polybrene or centrifugation. Twenty-four hours later, blasticidin (1.0 μg/ml) was added to the media. After selection, 1 × 10⁵ cells were plated on 60 mm dishes and treated 24 h later with 5 μM of etoposide. Standard retroviral techniques were used for assessment of the PEST sequence in MEFs. SAOS-2, HTB-9, and C33a cells were transfected using the calcium phosphate method. *Drosophila* Schneider 2 cells were transfected using nucleofector (Amaxa). Survival was quantified by flow cytometry using the Live/Dead kit (Molecular Probes) or by microplate reader at 450 nm using the Cell Counting kit-8 (Dojindo Molecular Technologies).

Immunoblotting and Immunoprecipitation

The following antibodies were used: anti-Bcl-x_L (610211) and anti-Bcl-2 (610538) from Transduction Laboratories; anti-Bcl-x_L (2764) from Cell Signaling; anti-tubulin (sc-9104), anti-actin (sc-1616), anti-Mcl-1 (sc-819), and anti-Ubiquitin (sc-8017) from Santa Cruz Biotechnology; anti-HSV-Tag (69171) from Novagen; and anti-HA (1867423) from Roche. Immunoblotting and immunoprecipitation were performed as previously described [16]. For immunoprecipitation, lysis buffer (50 mM HEPES (pH 7.0), 250 mM NaCl, 1 mM EDTA, 0.2% NP-40, and Complete Protease Inhibitor (Roche) was used.

Pulse Chase

Bcl-x_L-inducible SAOS-2 cells were induced by doxycycline treatment and pulsed with ³⁵S-methionine for 4 h. Cells treated with calpain inhibitor I as indicated and chased for the specified times. The cell lysates were prepared and immunoprecipitated for Bcl-x_L as described previously [16] and then analyzed by SDS-PAGE and autoradiography.

Intracellular pH Measurements

Cells were grown in a HEPES-buffered medium instead of the standard HCO₃⁻/CO₂ buffer system to avoid the rapid shifts in pH that occur when cells in the HCO₃⁻/CO₂ buffer system are removed from the 5% CO₂ atmosphere of an incubator. Sixty hours after DNA-damaging agent treatment, cells were washed with PBS. The studies were purposefully biased towards the assessment of cells in the earlier stages of apoptosis by measuring the pH of only those cells that remained adherent to the tissue culture dish. These cells were loaded with 5 μM of SNARF-1 for 10 min and then washed with PBS just prior to assessment by flow cytometry. The SNARF-1 was excited at 488 nm and emissions were read at 585 nm (pH-dependent) and 640 nm (pH-indepen-

dent). The pH-independent emission allows for the normalization of SNARF-1 loading differences between cells. The ratio of the emissions was calculated and the pH was read from a calibration curve. An in situ calibration curve was generated as follows: Cells are loaded with SNARF-1 as above. HEPES was used to make buffers at 0.5 pH unit intervals ranging from pH 6.5–8.5. These contained the ionophore nigericin 13 μM and K⁺ 140 mM to render the cells permeable to the buffers. Cells were equilibrated in the buffers for 20 min. The cells were then analyzed by flow cytometry, and a calibration curve of the pH versus the ratio of the pH-dependent and pH-independent emissions was plotted.

Supporting Information

Figure S1 Dataset used for MEME analysis. The sequences of the region between the BH4 and BH3 domains of the members of the Bcl-x_L homology group in the Bcl-2 database[29] that were used for the MEME analysis. Bcl-2 database IDs are listed. (PDF)

Figure S2 Deamidation has no effect on the interaction of Bcl-x_L with Bim or Bax. (A) Immunoblot for endogenous Bcl-x_L in whole cell lysates and either IgG (control) or anti-Bim immunoprecipitates from untreated and 10 μM of etoposide-treated C33a cells. We have previously demonstrated that the most rapidly migrating form of human Bcl-x_L during SDS-PAGE is the native form and the forms that migrate more slowly are deamidated at one or both sites [16]. (B) Bim expression was induced by doxycycline treatment of a Bim-inducible SAOS-2 cell line in which Bcl-x_L is constitutively overexpressed and an immunoblot was performed for the indicated proteins in whole cell lysates and either IgG or anti-Bim immunoprecipitates. Two different exposures of the immunoblot for the co-immunoprecipitated proteins are shown to facilitate the visualization of all of the forms of Bcl-x_L that are co-immunoprecipitated by different concentrations of Bim. That Bcl-x_L levels appear to increase after Bim expression is induced is most likely because the cells that express the highest levels of Bcl-x_L have a survival advantage once Bim is expressed. (C) The experiment outlined in (B) was repeated using cells that were treated with 10 μM of etoposide to induce further deamidation of Bcl-x_L. Etoposide treatment depresses the inducibility of Bim in these cells. (D) Immunoblot analysis of Bcl-x_L in whole cell lysates (left) and either anti-Bim or anti-HA immunoprecipitates (right) from C33a cells in which HA-tagged Bcl-x_L and untagged Bcl-x_L were expressed as indicated. The cells were treated with 10 μM of etoposide for 48 h. Both immunoprecipitations were performed using the same cell lysate. (E) GFP-Bax was expressed in a SAOS2 cell line in which Bcl-x_L is constitutively overexpressed and an

immunoblot was performed for the indicated proteins using whole cell lysates and either IgG or anti-GFP immunoprecipitates. Two different exposures of the immunoblot for the co-immunoprecipitated proteins are shown to facilitate the visualization of all of the forms of Bcl-x_L that are co-immunoprecipitated by different concentrations of the anti-GFP antibody. (TIF)

Figure S3 Bcl-x_L deamidation is regulated by cytosolic pH. (A) Immunoblot of Bcl-x_L in SAOS-2 cell lysates that were incubated at pH 7.2, pH 7.4, or pH 7.6 for the indicated times. (B) Immunoblot of Bcl-x_L from intact C33a, HTB-9, and SAOS-2 cells that were incubated in tissue culture medium at pH 6.5 or pH 7.3 and treated with 10 μM of monensin as indicated. (C) Immunoblot of purified bacterially synthesized wild-type Bcl-x_L and Bcl-x_L(N52A/N66A) that was incubated at pH 7.2, pH 7.4, or pH 7.6 for the indicated times. (D) SAOS-2 cells were treated with the indicated DNA-damaging agents. The percent of adherent cells with a pH above an arbitrarily chosen value of approximately pH 7.3 is indicated. (TIF)

Table S1 Genbank accession numbers for Bcl-x_L-like proteins. Genbank accession numbers for the proteins in Figures 1B and 2B are listed. (DOCX)

Text S1 Deamidation has no effect on the interaction of Bcl-x_L with Bim or Bax. (DOCX)

Text S2 DNA damage-induced Bcl-x_L deamidation is regulated by changes in pH in the cell. (DOCX)

Acknowledgments

We thank K. Grapperhaus for technical support. We are grateful to Dr. Peter Greer for providing *Capn4*^{-/-} and rescued *Capn4*^{-/-} MEFs. We also thank Drs. Kyu-Sun Lee and Kyung-Ok Cho for providing pCMA plasmid and *Drosophila* Schneider 2 cells.

Author Contributions

The author(s) have made the following declarations about their contributions: Conceived and designed the experiments: SJW SHD BED SRM CL. Performed the experiments: SJW SHD BED SRM CL LG JJR. Analyzed the data: SJW SHD BED CL SRM LG JJR RA. Contributed reagents/materials/analysis tools: CL RA KSK. Wrote the paper: SJW SHD BED SRM CL.

References

1. Youle RJ, Strasser A (2008) The BCL-2 protein family: opposing activities that mediate cell death. *Nat Rev Mol Cell Biol* 9: 47–59.
2. Korsmeyer SJ, Shutter JR, Veis DJ, Merry DE, Oltvai ZN (1993) Bcl-2/Bax: a rheostat that regulates an anti-oxidant pathway and cell death. *Semin Cancer Biol* 4: 327–332.
3. Adams JM, Cory S (2007) The Bcl-2 apoptotic switch in cancer development and therapy. *Oncogene* 26: 1324–1337.
4. Friess H, Lu Z, Andren-Sandberg A, Berberat P, Zimmermann A, et al. (1998) Moderate activation of the apoptosis inhibitor bcl-xL worsens the prognosis in pancreatic cancer. *Ann Surg* 228: 780–787.
5. Martinez-Brocca MA, Castilla C, Navarro E, Amaya MJ, Travado P, et al. (2008) Clinicopathological correlations of Bcl-xL and Bax expression in differentiated thyroid carcinoma. *Clin Endocrinol (Oxf)* 68: 190–197.
6. Zhao WL, Daneshpouy ME, Mounier N, Briere J, Leboeuf C, et al. (2004) Prognostic significance of bcl-xL gene expression and apoptotic cell counts in follicular lymphoma. *Blood* 103: 695–697.
7. Materna V, Surowiak P, Markwitz E, Spaczynski M, Drag-Zalesinska M, et al. (2007) Expression of factors involved in regulation of DNA mismatch repair- and apoptosis pathways in ovarian cancer patients. *Oncol Rep* 17: 505–516.
8. Williams J, Lucas PC, Griffith KA, Choi M, Fogoros S, et al. (2005) Expression of Bcl-xL in ovarian carcinoma is associated with chemoresistance and recurrent disease. *Gynecol Oncol* 96: 287–295.
9. Watanabe J, Kushihata F, Honda K, Sugita A, Tateishi N, et al. (2004) Prognostic significance of Bcl-xL in human hepatocellular carcinoma. *Surgery* 135: 604–612.
10. Castilla C, Congregado B, Chinchon D, Torrubia FJ, Japon MA, et al. (2006) Bcl-xL is overexpressed in hormone-resistant prostate cancer and promotes survival of LNCaP cells via interaction with proapoptotic Bak. *Endocrinology* 147: 4960–4967.
11. Aebersold DM, Kollar A, Beer KT, Laissue J, Greiner RH, et al. (2001) Involvement of the hepatocyte growth factor/scatter factor receptor c-met and of Bcl-xL in the resistance of oropharyngeal cancer to ionizing radiation. *Int J Cancer* 96: 41–54.
12. Amundson SA, Myers TG, Scudiero D, Kitada S, Reed JC, et al. (2000) An informatics approach identifying markers of chemosensitivity in human cancer cell lines. *Cancer Res* 60: 6101–6110.
13. Minn AJ, Rudin CM, Boise LH, Thompson CB (1995) Expression of bcl-xL can confer a multidrug resistance phenotype. *Blood* 86: 1903–1910.

14. Shoemaker AR, Oleksijew A, Bauch J, Belli BA, Borre T, et al. (2006) A small-molecule inhibitor of Bcl-XL potentiates the activity of cytotoxic drugs in vitro and in vivo. *Cancer Res* 66: 8731–8739.
15. Littlejohn JE, Cao X, Miller SD, Ozvaran MK, Jupiter D, et al. (2008) Bcl-xL antisense oligonucleotide and cisplatin combination therapy extends survival in SCID mice with established mesothelioma xenografts. *Int J Cancer* 123: 202–208.
16. Deverman BE, Cook BL, Manson SR, Niederhoff RA, Langer EM, et al. (2002) Bcl-xL deamidation is a critical switch in the regulation of the response to DNA damage. *Cell* 111: 51–62.
17. Henderson CC, Zhang Z, Manson SR, Richm JJ, Kataoka M, et al. (2005) A moderate reduction of Bcl-x(L) expression protects against tumorigenesis; however, it also increases susceptibility to tissue injury. *Oncogene* 24: 7120–7124.
18. Zhang H, Taylor J, Luther D, Johnston J, Murray S, et al. (2003) Antisense oligonucleotide inhibition of Bcl-xL and Bid expression in liver regulates responses in a mouse model of Fas-induced fulminant hepatitis. *J Pharmacol Exp Ther* 307: 24–33.
19. de la Coste A, Fabre M, McDonell N, Porteu A, Gilgenkrantz H, et al. (1999) Differential protective effects of Bcl-xL and Bcl-2 on apoptotic liver injury in transgenic mice. *Am J Physiol* 277: G702–G708.
20. Kamimukai N, Togo S, Hasegawa S, Kubota T, Kurosawa H, et al. (2001) Expression of Bcl-2 family reduces apoptotic hepatocytes after excessive hepatectomy. *Eur Surg Res* 33: 8–15.
21. Tsang SP, Fausto N, Hockenbery DM (1997) Expression of Bcl-2 family during liver regeneration and identification of Bcl-x as a delayed early response gene. *Am J Pathol* 150: 1985–1995.
22. Iravani S, Zhang HQ, Yuan ZQ, Cheng JQ, Karl RC, et al. (2003) Modification of insulin-like growth factor 1 receptor, c-Src, and Bcl-XL protein expression during the progression of Barrett's neoplasia. *Hum Pathol* 34: 975–982.
23. Zhao R, Yang FT, Alexander DR (2004) An oncogenic tyrosine kinase inhibits DNA repair and DNA-damage-induced Bcl-xL deamidation in T cell transformation. *Cancer Cell* 5: 37–49.
24. Chang CY, Lin YM, Lee WP, Hsu HH, Chen EI (2006) Involvement of Bcl-X(L) deamidation in E1A-mediated cisplatin sensitization of ovarian cancer cells. *Oncogene* 25: 2656–2665.
25. Robinson NE, Robinson AB (2001) Prediction of protein deamidation rates from primary and three-dimensional structure. *Proc Natl Acad Sci U S A* 98: 4367–4372.
26. Muchmore SW, Sattler M, Liang H, Meadows RP, Harlan JE, et al. (1996) X-ray and NMR structure of human Bcl-xL, an inhibitor of programmed cell death. *Nature* 381: 335–341.
27. Bryson K, McGuffin LJ, Marsden RL, Ward JJ, Sodhi JS, et al. (2005) Protein structure prediction servers at University College London. *Nucleic Acids Res* 33: W36–W38.
28. Cuff JA, Clamp ME, Siddiqui AS, Finlay M, Barton GJ (1998) JPred: a consensus secondary structure prediction server. *Bioinformatics* 14: 892–893.
29. Blaineau SV, Aouacheria A (2009) BCL2DB: moving 'helix-bundled' BCL2 family members to their database. *Apoptosis: An International Journal on Programmed Cell Death* 14: 923–925.
30. Bailey TL, Williams N, Misleh C, Li WW (2006) MEME: discovering and analyzing DNA and protein sequence motifs. *Nucleic Acids Research* 34: W369–W373.
31. Hertz GZ, Stormo GD (1999) Identifying DNA and protein patterns with statistically significant alignments of multiple sequences. *Bioinformatics* 15: 563–577.
32. Bailey TL (2002) Discovering novel sequence motifs with MEME. *Curr Protoc Bioinformatics Chapter 2: Unit 2.4*.
33. Robinson NE, Robinson ZW, Robinson BR, Robinson AL, Robinson JA, et al. (2004) Structure-dependent nonenzymatic deamidation of glutaminyl and asparaginyl pentapeptides. *The Journal of Peptide Research* 63: 426–436.
34. Zhao R, Follows GA, Beer PA, Scott LM, Huntly BJ, et al. (2008) Inhibition of the Bcl-xL deamidation pathway in myeloproliferative disorders. *N Engl J Med* 359: 2778–2789.
35. Takehara T, Takahashi H (2003) Suppression of Bcl-xL deamidation in human hepatocellular carcinomas. *Cancer Res* 63: 3054–3057.
36. Deverman BE, Cook BL, Manson SR, Niederhoff RA, Langer EM, et al. (2003) Erratum to: Bcl-xL deamidation is a critical switch in the regulation of the response to DNA damage. *Cell* 115: 503.
37. Zhao R, Oxley D, Smith TS, Follows GA, Green AR, et al. (2006) DNA damage-induced Bcl-xL deamidation is mediated by NHE-1 antiporter regulated intracellular pH. *PLoS Biol* 5: e1. doi:10.1371/journal.pbio.0050001
38. Chang BS, Minn AJ, Muchmore SW, Fesik SW, Thompson CB (1997) Identification of a novel regulatory domain in Bcl-X(L) and Bcl-2. *Embo J* 16: 968–977.
39. Aritomi M, Kunishima N, Inohara N, Ishibashi Y, Ohta S, et al. (1997) Crystal structure of rat Bcl-xL. Implications for the function of the Bcl-2 protein family. *J Biol Chem* 272: 27886–27892.
40. Lo SC, Hannink M (2006) PGAM5, a Bcl-XL-interacting protein, is a novel substrate for the redox-regulated Keap1-dependent ubiquitin ligase complex. *J Biol Chem* 281: 37893–37903.
41. Chipuk JE, Kuwana T, Bouchier-Hayes L, Droin NM, Newmeyer DD, et al. (2004) Direct activation of Bax by p53 mediates mitochondrial membrane permeabilization and apoptosis. *Science* 303: 1010–1014.
42. Mihara M, Erster S, Zaika A, Petrenko O, Chittenden T, et al. (2003) p53 has a direct apoptogenic role at the mitochondria. *Mol Cell* 11: 577–590.
43. Schuler M, Maurer U, Goldstein JC, Breitenbucher F, Hoffarth S, et al. (2003) p53 triggers apoptosis in oncogene-expressing fibroblasts by the induction of Noxa and mitochondrial Bax translocation. *Cell Death Differ* 10: 451–460.
44. Minn AJ, Kettlun CS, Liang H, Kelekar A, Vander Heiden MG, et al. (1999) Bcl-xL regulates apoptosis by heterodimerization-dependent and -independent mechanisms. *EMBO J* 18: 632–643.
45. Minn AJ, Velez P, Schendel SL, Liang H, Muchmore SW, et al. (1997) Bcl-x(L) forms an ion channel in synthetic lipid membranes. *Nature* 385: 353–357.
46. Vander Heiden MG, Chandel NS, Williamson EK, Schumacker PT, Thompson CB (1997) Bcl-xL regulates the membrane potential and volume homeostasis of mitochondria. *Cell* 91: 627–637.
47. Koury MJ, Koury ST, Kopsombut P, Bondurant MC (2005) In vitro maturation of nascent reticulocytes to erythrocytes. *Blood* 105: 2168–2174.
48. Cimmino A, Capasso R, Muller F, Sambri I, Masella L, et al. (2008) Protein isoaspartate methyltransferase prevents apoptosis induced by oxidative stress in endothelial cells: role of Bcl-XI deamidation and methylation. *PLoS One* 3: e3258. doi:10.1371/journal.pone.0003258
49. Rechsteiner M, Rogers SW (1996) PEST sequences and regulation by proteolysis. *Trends Biochem Sci* 21: 267–271.
50. Rogers S, Wells R, Rechsteiner M (1986) Amino acid sequences common to rapidly degraded proteins: the PEST hypothesis. *Science* 234: 364–368.
51. Thorsness PE, Koshland DE, Jr. (1987) Inactivation of isocitrate dehydrogenase by phosphorylation is mediated by the negative charge of the phosphate. *J Biol Chem* 262: 10422–10425.
52. Liu Z, Wang S, Zhou H, Yang Y, Zhang M (2009) Na⁺/H⁺ exchanger mediates TNF-alpha-induced hepatocyte apoptosis via the calpain-dependent degradation of Bcl-xL. *J Gastroenterol Hepatol* 24: 879–885.
53. Nakagawa T, Yuan J (2000) Cross-talk between two cysteine protease families. Activation of caspase-12 by calpain in apoptosis. *J Cell Biol* 150: 887–894.
54. Gil-Parrado S, Fernandez-Montalvan A, Assalg-Machleidt I, Popp O, Bestvater F, et al. (2002) Ionomycin-activated calpain triggers apoptosis. A probable role for Bcl-2 family members. *J Biol Chem* 277: 27217–27226.
55. Martinez LO, Agerholm-Larsen B, Wang N, Chen W, Tall AR (2003) Phosphorylation of a pest sequence in ABCA1 promotes calpain degradation and is reversed by ApoA-I. *J Biol Chem* 278: 37368–37374.
56. Shumway SD, Maki M, Miyamoto S (1999) The PEST domain of IkappaBalpha is necessary and sufficient for in vitro degradation by mu-calpain. *J Biol Chem* 274: 30874–30881.
57. Wang N, Chen W, Linsel-Nitschke P, Martinez LO, Agerholm-Larsen B, et al. (2003) A PEST sequence in ABCA1 regulates degradation by calpain protease and stabilization of ABCA1 by apoA-I. *J Clin Invest* 111: 99–107.
58. Fujita N, Nagahashi A, Nagashima K, Rokudai S, Tsuruo T (1998) Acceleration of apoptotic cell death after the cleavage of Bcl-XL protein by caspase-3-like proteases. *Oncogene* 17: 1295–1304.
59. Tan Y, Wu C, De Veyra T, Greer PA (2006) Ubiquitous calpains promote both apoptosis and survival signals in response to different cell death stimuli. *J Biol Chem* 281: 17689–17698.
60. Gottlieb RA, Nordberg J, Skowronski E, Babior BM (1996) Apoptosis induced in Jurkat cells by several agents is preceded by intracellular acidification. *Proc Natl Acad Sci U S A* 93: 654–658.
61. Matsuyama S, Llopis J, Deveraux QL, Tsien RY, Reed JC (2000) Changes in intramitochondrial and cytosolic pH: early events that modulate caspase activation during apoptosis. *Nat Cell Biol* 2: 318–325.
62. Zhu WH, Loh TT (1995) Effects of Na⁺/H⁺ antiporter and intracellular pH in the regulation of HL-60 cell apoptosis. *Biochim Biophys Acta* 1269: 122–128.
63. Grenier AL, Abu-ihweij K, Zhang G, Ruppert SM, Boohaker R, et al. (2008) Apoptosis-induced alkalization by the Na⁺/H⁺ exchanger isoform 1 is mediated through phosphorylation of amino acids Ser726 and Ser729. *Am J Physiol Cell Physiol* 295: C883–896.
64. Tsao N, Lei HY (1996) Activation of the Na⁽⁺⁾/H⁽⁺⁾ antiporter, Na⁺/HCO₃⁽⁻⁾/CO₃⁽²⁻⁾ cotransporter, or Cl⁽⁻⁾/HCO₃⁽⁻⁾ exchanger in spontaneous thymocyte apoptosis. *J Immunol* 157: 1107–1116.
65. Dai HY, Tsao N, Leung WC, Lei HY (1998) Increase of intracellular pH in p53-dependent apoptosis of thymocytes induced by gamma radiation. *Radiat Res* 150: 183–189.
66. Khaled AR, Moor AN, Li A, Kim K, Ferris DK, et al. (2001) Trophic factor withdrawal: p38 mitogen-activated protein kinase activates NHE1, which induces intracellular alkalization. *Mol Cell Biol* 21: 7545–7557.
67. Huc L, Sparfel L, Rissel M, Dimanche-Boitrel MT, Guillouzo A, et al. (2004) Identification of Na⁺/H⁺ exchange as a new target for toxic polycyclic aromatic hydrocarbons. *Faseb J* 18: 344–346.
68. Robinson NE (2002) Protein deamidation. *Proc Natl Acad Sci U S A* 99: 5283–5288.
69. Flatmark T, Sletten K (1968) Multiple forms of cytochrome c in the rat. Precursor-product relationship between the main component Cy I and the minor components Cy II and Cy III in vivo. *J Biol Chem* 243: 1623–1629.
70. Watanabe A, Takio K, Ihara Y (1999) Deamidation and isoaspartate formation in smeared tau in paired helical filaments. Unusual properties of the microtubule-binding domain of tau. *J Biol Chem* 274: 7368–7378.
71. Takemoto L, Emmons T, Granstrom D (1990) The sequences of two peptides from cataract lenses suggest they arise by deamidation. *Curr Eye Res* 9: 793–797.

72. Reissner KJ, Aswad DW (2003) Deamidation and isoaspartate formation in proteins: unwanted alterations or surreptitious signals? *Cell Mol Life Sci* 60: 1281–1295.
73. Elledge SJ, Winston J, Harper JW (1996) A question of balance: the role of cyclin-kinase inhibitors in development and tumorigenesis. *Trends Cell Biol* 6: 388–392.
74. Robinson AB, Rudd CJ (1974) Deamidation of glutaminyl and asparaginyll residues in peptides and proteins. *Curr Top Cell Regul* 8: 247–295.
75. Wong JT (1975) A co-evolution theory of the genetic code. *Proc Natl Acad Sci U S A* 72: 1909–1912.
76. Marchler-Bauer A, Lu S, Anderson JB, Chitsaz F, Derbyshire MK, et al. (2011) CDD: a Conserved Domain Database for the functional annotation of proteins. *Nucleic Acids Research* 39: D225–D229.
77. Hu X, Cherbas L, Cherbas P (2003) Transcription activation by the ecdysone receptor (EcR/USP): identification of activation functions. *Mol Endocrinol* 17: 716–731.
78. Rice P, Longden I, Bleasby A (2000) EMBOSS: the European Molecular Biology Open Software Suite. *Trends Genet* 16: 276–277.